



DETERMINATION OF RESIDUAL WELDING STRESSES IN LOAD BEARING STRUCTURES MADE OF WELDED HOLLOW SECTIONS

Antanas Žiliukas¹, Andrius Surantas²

^{1,2}*Kaunas University of Technology, Strength and Fracture Mechanics Centre,
Kęstučio g. 27, 44025 Kaunas, Lithuania*
E-mails: ¹*antanas.ziliukas@ktu.lt* ; ²*andrius.surantas@gmail.com*

Abstract. This paper presents methodology for determining residual stresses originated from welding process in load bearing bridge steel structures made of square profile tubes. Simulated welding process was performed together with the selected welding sequences and due to significant thermal effect on the welding area residual stresses inside the butt weld area and around it were evaluated. The developed finite element (FE) model allows determining residual stresses of welding in any type of hollow sections butt welds.

Keywords: bridge steel structures, hollow sections, welding, welded joints, stress, strain, finite elements (FE), residual stress.

1. Introduction

Recently more and more hollow sections from structural steel are used as the main load bearing structures for bridges. Using those profiles makes structures light weighted, saves materials and empowers to build well-balanced and economic bridges.

Most popular standard profiles between hollow sections are square and rectangular tubes. Exploitation of steel bridges proves that highest risks of failure occur in welded joints. Local expansion and shrinkage during the welding process generates local stresses and deformations in welded joints and heat-affected zone.

Residual stresses summarize together with external loads and minimize load-bearing abilities as well as originate brittle-plastic fracture due to specificity of the structure geometry.

The effect of welding process to load bearing abilities in thin-walled cylinders was described in previous studies (Cheng, Finnie 1986). Curvature of welded joints was described in studies (Teng *et al.* 2002). Residual stresses of welding were analyzed by (Jang *et al.* 2001). Finite element (FE) modeling methodology was described by Kiselev (1998), Медведев (2001), Grigorjeva *et al.* (2008) and Ziari *et al.* (2007).

However, welded joints in square tubes are studied like simply welded plates due to the specific geometry. Comparable studies were made by Wimpory *et al.* (2003) and Makhenko *et al.* (2006).

FE modeling was chosen for residual welding stresses in square profile tube butt joints. As described later, this

method allows changing tube profile, welded joint geometry, welding sequence, and material properties. This enables detailed evaluation of technological process and joint geometry.

2. Finite element model

Calculations were made in two stages. During stage 1 non-stationary task was solved. Here, the temperature field around welding area during and after the welding process was calculated. In stage 2 the strength calculations of welded joint determining stresses during the welding and residual stresses after the joint cooled down to room temperature were made.

For calculating temperature field the FE model consisting from 19824 SOLID70 type finite elements (98932 nodes) was developed. FE model of welded joint split to elements, and fragment of welded joint are shown in Fig. 1.

Thermal calculations were performed in 20 steps. First 19 steps were the simulation of welding process and the last step - cooling after final welding step. Welding sequence was simulated according to Fig. 2.

Each side of the tube was heated in four steps, and a welding period for one side made 12 s. Strength analysis was proportionately performed in 20 steps, respectively determining movements, deformations, and stresses. After the last step, temperature in all nodes was computed equal to 25 °C.

While using FE method the calculated results were highly dependent on how exactly mechanical properties of the material were described. This is extremely impor-

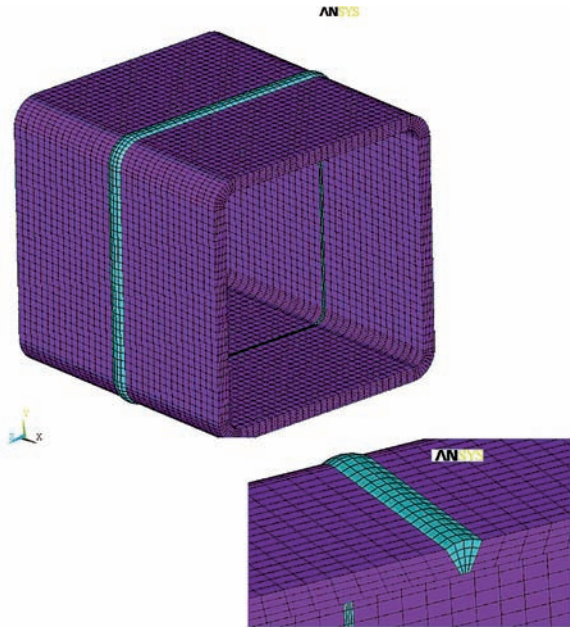


Fig. 1. FE model of welded joint

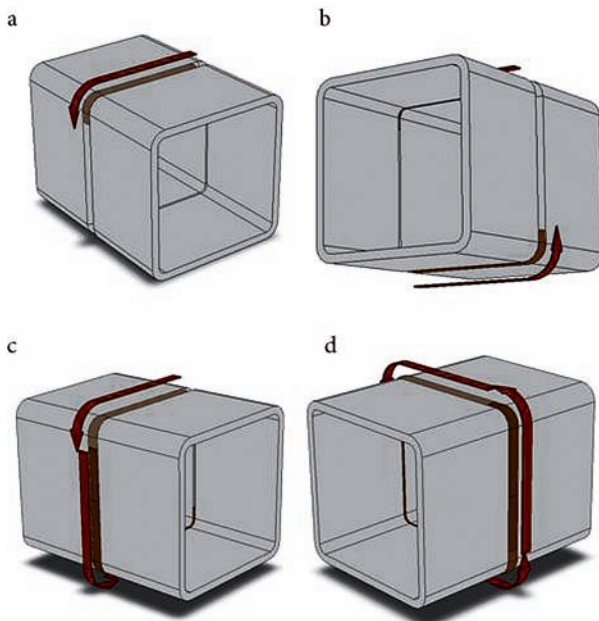


Fig. 2. Modelled sequence of tube butt joint welding

tant as these properties vary in the calculated range of temperatures. Using catalogues, those properties were found for pure materials, or their main alloys. Solving this model, mechanical properties of structural steel S355 J2 were needed in range of temperatures from 20 °C to 1500 °C (steel melting point).

Mechanical properties of structural steel S355 J2 were taken from Eurocode 3. Thermal conductivity, specific heat, and enthalpy reliance on temperature are shown respectively in Figs 3–5.

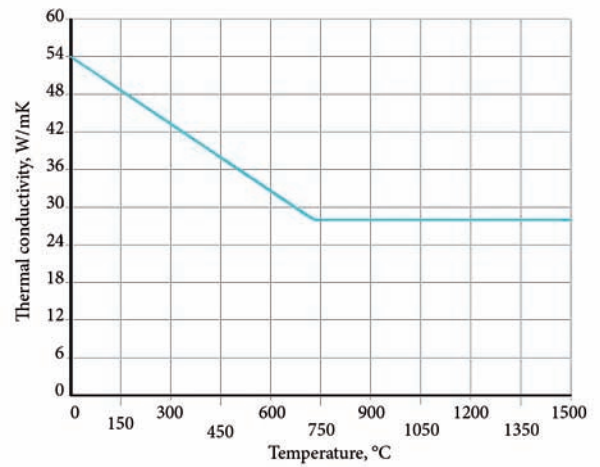


Fig. 3. Thermal conductivity reliance on temperature

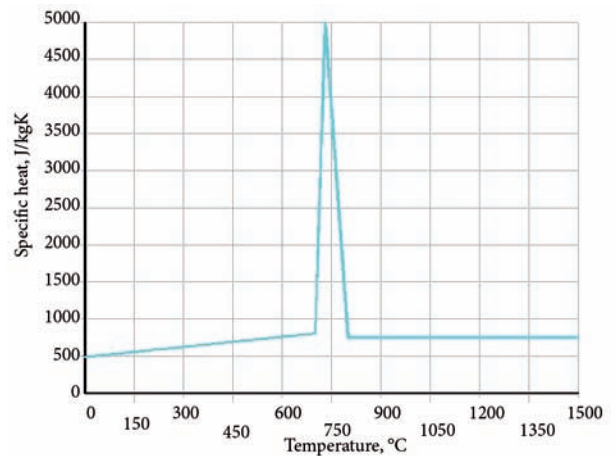


Fig. 4. Specific heat reliance on temperature

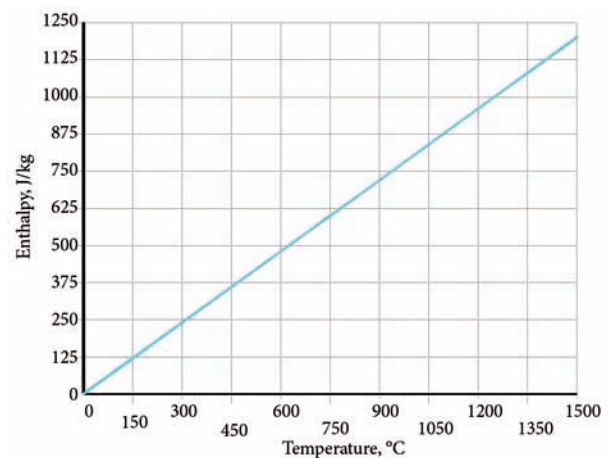


Fig. 5. Enthalpy reliance on temperature

Structural steel S355 J2 stress and strain dependence results were taken from the tests implemented by Outinen *et al.* (2001) and shown in Fig. 6.

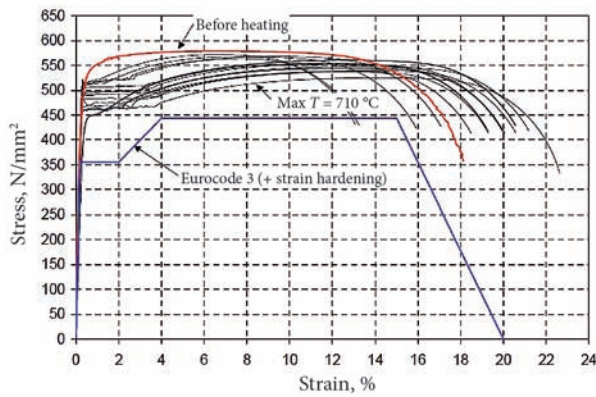


Fig. 6. Tensile test results of structural steel S355 J2

Fig. 7 shows Young’s module for steel S355 J2 reliance on temperature. Poisson’s ratio of main steel in full thermal ranges is taken equal to 0.3 and is the same as in welded joint.

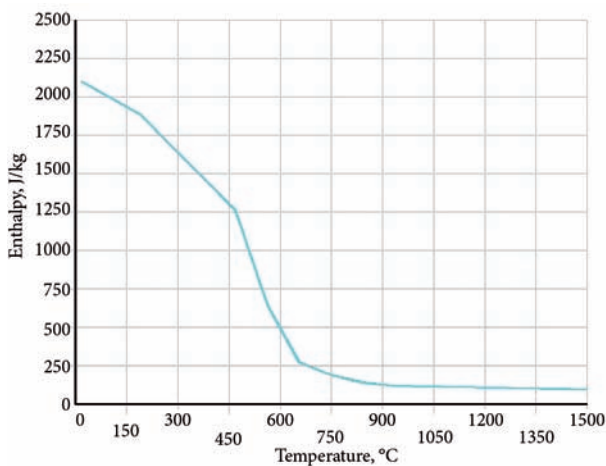


Fig. 7. Steel S355 J2 Young’s module reliance on temperature

3. Thermal fields of welded joints

Intermediate process of thermal field calculations takes the main part of calculations. FE formulation is presented below for describing variable thermal processes. Thermal balance equation of FE is as follows:

$$[K^e]\{T^e\} = \{S^e_\infty\} + \{P^e\} + \{Q^e\}, \quad (1)$$

where

$$[K^e] = \frac{\lambda A}{l} \begin{bmatrix} 1 & -1 \\ -1 & 1 \end{bmatrix} + \frac{\alpha pl}{2} \begin{bmatrix} 1 & 0 \\ 0 & 1 \end{bmatrix} + A\alpha_{g1} \begin{bmatrix} 1 & 0 \\ 0 & 0 \end{bmatrix} + A\alpha_{g2} \begin{bmatrix} 0 & 0 \\ 0 & 1 \end{bmatrix} \quad (2)$$

is thermal conductivity matrix for the element.

$$\{T^e\} = \begin{Bmatrix} T_1 \\ T_2 \end{Bmatrix} \text{ is vector of temperature in element nodes,} \quad (3)$$

$$\{S^e_\infty\} = \frac{\alpha pl T_\infty}{2} \begin{Bmatrix} 1 \\ 1 \end{Bmatrix} + \alpha_{g1} AT_\infty \begin{Bmatrix} 1 \\ 0 \end{Bmatrix} + \alpha_{g2} AT_\infty \begin{Bmatrix} 0 \\ 1 \end{Bmatrix} \quad (4)$$

is thermal power vector for the element caused by convection.

$$\{P^e\} = \frac{bAl}{2} \begin{Bmatrix} 1 \\ 1 \end{Bmatrix} \quad (5)$$

is thermal power vector for the element caused by volumetric heat sources.

$$\{Q^e\} = \begin{Bmatrix} Q_1 \\ Q_2 \end{Bmatrix} \quad (6)$$

is thermal power vector for the element received from nearby elements.

Eq (1) describes stationary (constant in time) thermal conductivity process. Solving this equation yields temperature settlement during the long period on various nodes of the element, as conditions of heat source and heat exchange with surroundings are determined.

This process flow in time is described by non-stationary equation for thermal conductivity. It is necessary to know two more physical constants for the material: specific heat, and density.

In Eq (1), additional members are filled as caused by element heat capacity. We admit beam temperature is non-stationary and in any of its cross-sections x vary with speed:

$$\frac{\partial T(x)}{\partial t} = \dot{T}(x). \quad (7)$$

This process is possible as any small segment of the beam length dx additionally is supported by heat power proportionally of beam part capacity $A dx$, and temperature decreasing speed $T(x)$.

Heat power applied to whole beam is equal to:

$$A \int_0^l cp \dot{T}(x) dx = cpAl \frac{\dot{T}_1 + \dot{T}_2}{2}. \quad (8)$$

This heat power is distributed to nodes of discrete element:

$$\frac{cpAl}{2} \begin{bmatrix} 1 & 0 \\ 0 & 1 \end{bmatrix} \begin{Bmatrix} \dot{T}_1 \\ \dot{T}_2 \end{Bmatrix} + \left(\frac{\lambda A}{l} \begin{bmatrix} 1 & -1 \\ -1 & 1 \end{bmatrix} + \frac{\alpha pl}{2} \begin{bmatrix} 1 & 0 \\ 0 & 1 \end{bmatrix} + A_{g1} \alpha_{g1} \begin{bmatrix} 1 & 0 \\ 0 & 0 \end{bmatrix} + \left(A_{g2} \alpha_{g2} \begin{bmatrix} 0 & 0 \\ 0 & 1 \end{bmatrix} \right) \right) \begin{Bmatrix} T_1 \\ T_2 \end{Bmatrix} = \frac{\alpha pl T_\infty}{2} \begin{Bmatrix} 1 \\ 1 \end{Bmatrix} + \alpha_{g1} AT_\infty \begin{Bmatrix} 1 \\ 0 \end{Bmatrix} + \alpha_{g2} AT_\infty \begin{Bmatrix} 0 \\ 1 \end{Bmatrix} + \frac{bAl}{2} \begin{Bmatrix} 1 \\ 1 \end{Bmatrix} + \begin{Bmatrix} Q_1 \\ Q_2 \end{Bmatrix}. \quad (9)$$

And described as matrix:

$$[C^e]\{\dot{T}^e\} + [K^e]\{T^e\} = \{S^e_\infty\} + \{P^e\} + \{Q^e\}, \quad (10)$$

where

$$[C^e] = \frac{cpAl}{2} \begin{bmatrix} 1 & 0 \\ 0 & 1 \end{bmatrix} \text{ is heat capacity matrix for the element.}$$

Element heat capacity matrixes are collected into structure matrix according to known general rules, and non-stationary thermal balance equation is:

$$[C]\{\dot{T}\} + [K]\{T\} = \{S_\infty\} + \{P\} + \{Q\}. \quad (11)$$

Eq (11) is usually solved by numerical integration.

In this study most famous FE system ANSYS is chosen for describing transitional thermal processes according to the adopted algorithm.

Algorithm for the chosen task is very similar:

- for pre-processor system, geometrical model was made in a way that was possible to change its geometry, and materials. Splitting to FE and calculating model was made;
- most suitable solver is chosen where boundary conditions are set;
- for post-processor system, received results are being analyzed.

Executed thermal calculations of intermediate processes with FE method boundary conditions are described by heat release coefficient, temperature of surrounding and primary temperature of the model. Further, a method on heat release coefficient calculation is presented. Subject of chosen model is a structural steel tube, dimensions 60×60×3 mm, with steel grade S355J2. Total heat release coefficient is calculated taking into account the forced and natural convection and radiation.

3.1. Evaluating radiation in calculations of total heat release coefficient

Radiation heat interchanges between surface of steel ($T_L = \text{const.}$) and isothermal surroundings ($T_a = \text{const.}$) are described in Eq (12):

$$\alpha_r = 4\epsilon_{12}\sigma_0 T_L^3, \text{ W/m}^2\text{K}. \quad (12)$$

System blackness level evaluation:

$$\epsilon_{12} = \frac{1}{\frac{1}{\epsilon_1} + \frac{1}{\epsilon_2} - 1} = \frac{1}{\frac{1}{0.68} + \frac{1}{0.15} - 1} = 0.14. \quad (13)$$

Radiation constant:

$$\sigma_0 = 5.67 \times 10^{-8}, \text{ W/m}^2\text{K}^4. \quad (14)$$

Thus,

$$\alpha_r = 4 \times 0.14 \times 5.67 \times 10^{-8} T_L^3, \text{ W/m}^2\text{K}. \quad (15)$$

Formed glass temperature decrease is assessed by the following differential equation:

$$-mc_p dT_s = \alpha F (T_s - T_a) dt, \quad (16)$$

$$K_a = \frac{mc_p}{\alpha F} = \frac{10 \times 1500}{200 \times 0.37 \times 0.37} \cong 550. \quad (17)$$

Thus, differential equation:

$$-\frac{dt}{550} = \frac{dT_s}{T_s - T_a}. \quad (18)$$

With integration limits:

$$t \rightarrow 0 \div t,$$

$$T_s \rightarrow T_L \div T_s$$

is obtained

$$T_s = T_a + (T_L - T_a) \exp\left(-\frac{t}{K_a}\right) \quad (19)$$

or

$$T_s = T_a + (T_L - T_a) \exp\left(-\frac{t}{550}\right). \quad (20)$$

Inserting T_s instead of T_L yields:

$$\alpha_r = 3.175 \times 10^{-8} \left[273 + (T_L - 273) \times \exp\left(-\frac{t}{550}\right) \right]^3, \quad (21)$$

where t – seconds; T_L – steel melting point.

3.2. Convective heat exchange evaluation when calculating total heat release coefficient

Suppose steel plate with width varying by axis x , airflow with speed w_0 is supplied. Airflow speed on the surface of steel plate is w_x .

Then

$$\frac{\alpha_x x}{\lambda_0} = 0.332 \times P_{ro}^{\frac{1}{3}} \times R_{ex}^{\frac{1}{2}}, \quad (22)$$

where

$$R_{ex} = \frac{w_x x}{\nu_0} \quad (23)$$

and

$$\lambda_0 = 0.025, \text{ W/mK}.$$

Used known values are as follows:

$$0.332 \frac{0.72 \times \frac{1}{3} \times 0.025}{3}, \quad (15 \times 10^{-6})^{\frac{1}{2}}$$

admitting the following

$$w_x = w_0 \left(\frac{r_0}{x} \right)^2. \quad (24)$$

Thus,

$$\alpha_x = 1.86 \times \frac{1}{x} (w_x \times x)^{\frac{1}{2}}, \quad (25)$$

and

$$\alpha_x = 1.86 \times w_0^2 \times \left(\frac{d_0}{2}\right) \times \frac{1}{x^{2.5}}, \quad (26)$$

where

$$x = r_0, \text{ with } x < r_0.$$

3.3. Evaluation of shield heat exchange by natural convection (caused by ΔT) when calculating total heat release coefficient

Supposing d_e is the measure that occurs from convection when surrounding environment is air, $P_r = 0.7$.

$$N_u = 0.429 \times G_r^{\frac{1}{4}},$$

$$N_u = \frac{\alpha_n \times d_e}{\alpha_0} - \text{Nuselt number}, \quad (27)$$

$$G_r = \frac{g \times d_e^3 \times \beta \times \Delta T}{\nu_0^2} - \text{Grasghof number}, \quad (28)$$

where $\lambda_0 = 0.025 \text{ W/mK}$; $\nu_0 = 15 \times 10^{-6} \text{ m}^2/\text{s}$; $g = 9.81 \text{ m/s}^2$; $\beta = 1/273 \text{ 1/K}$.

Thus,

$$\alpha_n = \lambda_0 \times 0.429 \times \left(\frac{g \times \beta}{\nu_0^2}\right)^{\frac{1}{4}} \times (\Delta T)^{\frac{1}{4}} \times d_e^{-\frac{1}{4}}. \quad (29)$$

Therefore,

$$\alpha_n = 1.206 \left[(T_L - 273) \exp\left(-\frac{t}{550}\right) \right]^{\frac{1}{4}} d_e^{-\frac{1}{4}}. \quad (30)$$

As shown, total heat release coefficient evaluating natural and forced convection and radiation is described:

$$\begin{aligned} \alpha_s &= \alpha_n + \alpha_x + \alpha_r = \\ &1.206 \left[(T_L - 273) \exp\left(-\frac{t}{550}\right) \right]^{\frac{1}{4}} d_e^{-\frac{1}{4}} + \\ &1.86 \times w_0^2 \times \left(\frac{d_0}{2}\right) \times \frac{1}{x^{2.5}} + \\ &3.175 \times 10^{-8} \left[273 + (T_L - 273) \exp\left(-\frac{t}{550}\right) \right]^3. \end{aligned} \quad (31)$$

Considering that Eq (31) has several variable values (time, coordinates, airflow speed) with the help of MATLAB software package ruling program for calculations of total heat release coefficient on various places of the model, according to the surrounding conditions and the forced cooling conditions in certain period was made.

3.4. Thermal fields of defect-free welded joints

Thermal fields of welded tube butt joint were calculated in three cooling modes: intensive, average and slow. Highest differences in temperatures were noticed as intensive temperature decrease in welded joint was performed.

Figs 8–13 show thermal fields in and around welded joint as welding process simulation is performed.

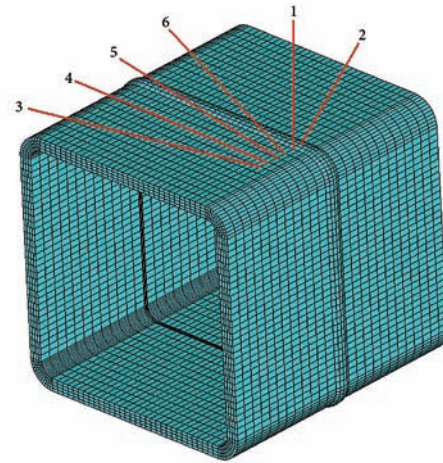


Fig. 8. Set control points (1–6) for temperature distribution

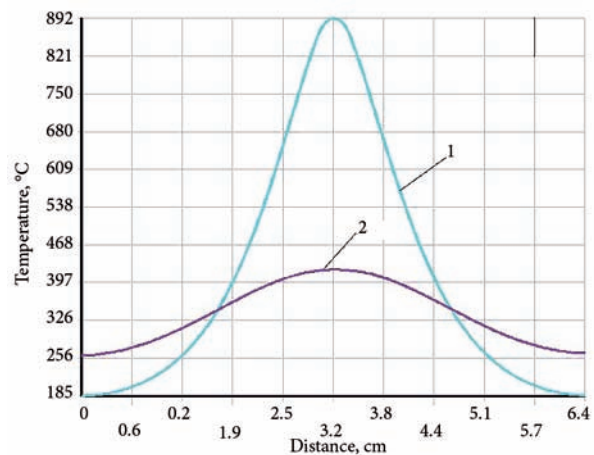


Fig. 9. Distribution of temperatures on control points: 1 – 10 s after welding; 2 – 20 s after welding

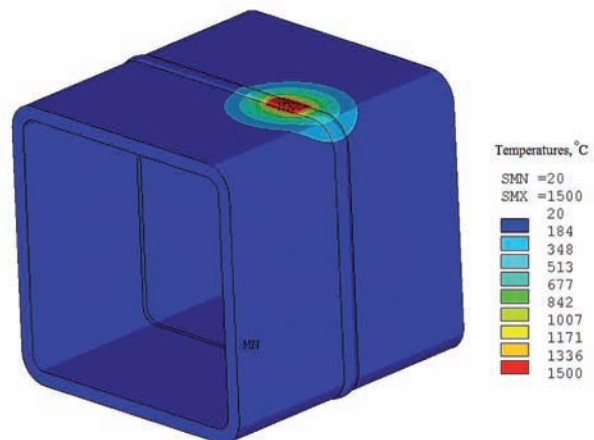


Fig. 10. Temperature distribution fields after 3 s from welding simulation has started

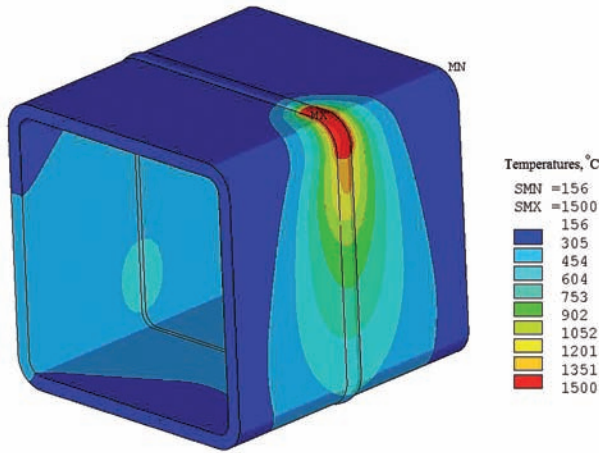


Fig. 11. Temperature distribution fields after 56 s from welding simulation has started

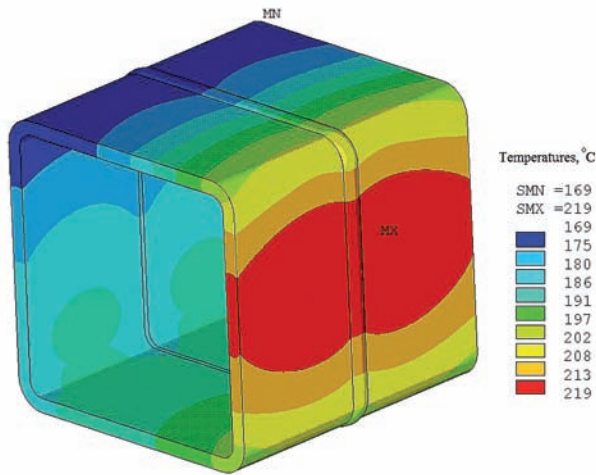


Fig. 12. Temperature distribution fields after 120 s from welding simulation has started

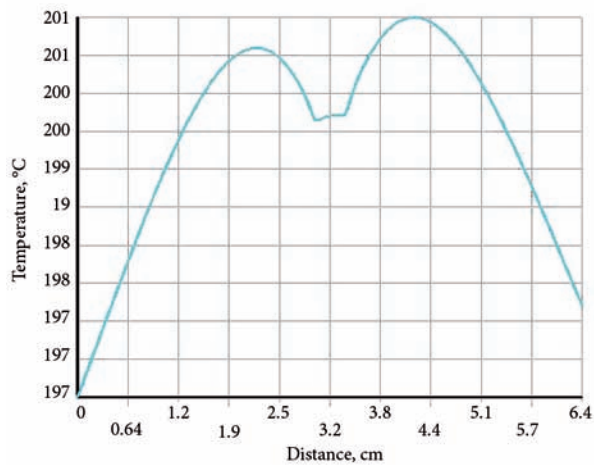


Fig. 13. Temperature distribution fields on control line points after 120 s from welding simulation has started

4. Residual stresses calculation results

In this section, results of welding residual stresses in defect-free tube butt joint are presented. Fig. 14 shows positions of coordinate axes regarding to welded joint geometry.

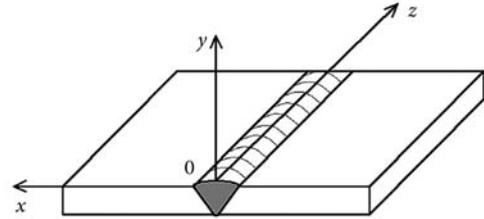


Fig. 14. Positions of coordinate axes regarding to welded joint

Figs 15–18 present results of residual welding stresses after welding process in tube butt joint.

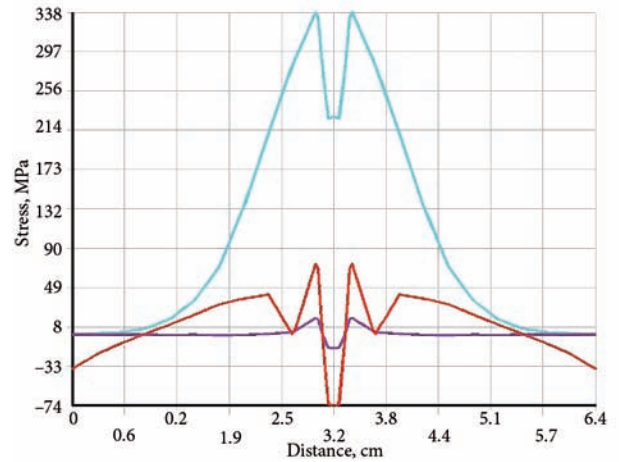


Fig. 15. Residual stresses distribution on control line points x , y and z axis-wise as joint is cooling down to room temperature, MPa

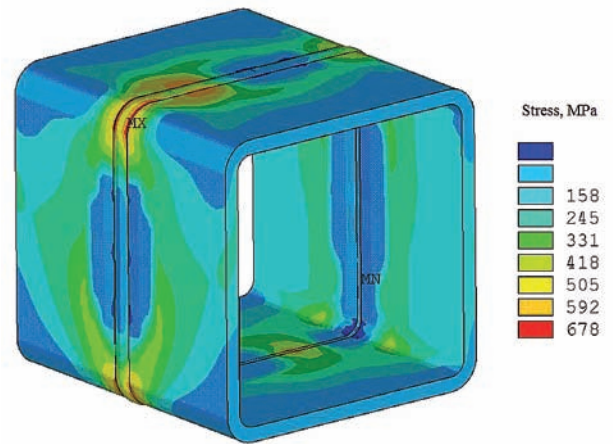


Fig. 16. Main residual stress σ_1 fields as joint is cooling down to room temperature, MPa

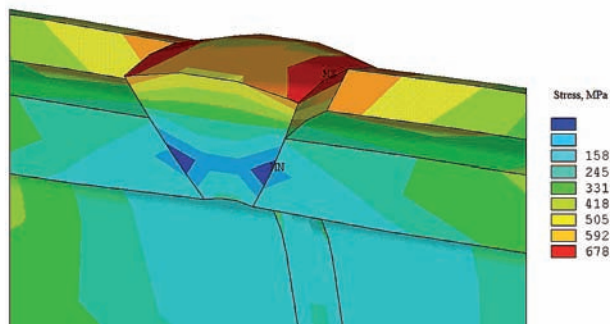


Fig. 17. Main residual stress σ_1 fields with maximized tube corner view, MPa

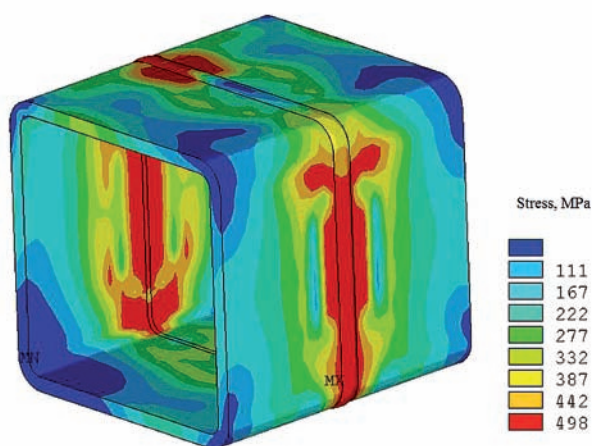


Fig. 18. Von Mises stress fields as joint is cooling down to room temperature, MPa

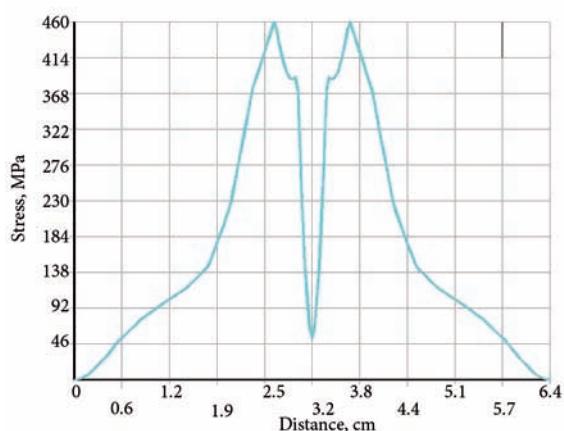


Fig. 19. Von Mises stress field distribution on control line points as joint is cooling down to room temperature, MPa

4. Conclusions

Using FE method, the distribution of temperatures in the various points of welding area was obtained. The process was described in a time flow. Total heat release process was calculated taking into account forced and natural convection and radiation. That enabled calculating heat release coefficient in various points of the model.

During calculations, different cooling modes were used: intensive, average and slow. Highest differences of temperatures were noticed when intensive cooling of welded joint was performed.

Welding residual stresses were calculated after joint welding process and cooling down to room temperature. The highest values of residual stresses were found on corners of tube butt joints. That shows high-risk areas in such kind of welded joints.

References

- Cheng, W.; Finnie, I. 1986. Measurement of Residual Hoop Stresses in Cylinders Using the Compliance Method, *Journal of Engineering Materials and Technology* 108(2): 87–92. doi:10.1115/1.3225864
- Grigorjeva, T.; Juozapaitis, A.; Kamaitis, Z.; Paeglitis, A. 2008. Finite Element Modeling for Static Behavior Analysis of Suspension Bridges with Varying Rigidity of Main Cables, *The Baltic Journal of Road and Bridge Engineering* 3(3): 121–128. doi:10.3846/1822-427X.2008.3.121-128
- Jang, G. B.; Kim, H. K.; Kang, S. S. 2001. Effect of Root Opening on Mechanical Properties, Deformation and Residual Stress of Weldments, *Welding Journal* 80(3):80–89.
- Kiselev, S. N.; Kiselev, A. S.; Kurkin, A.; Aladinskii, V. V.; Makhenko, V. O. 1999. Current Aspects of Computer Modelling Thermal and Deformation Stresses and Structure Formation in Welding and Related Technologies, *Welding International* 13(4): 314–322. doi:10.1080/09507119909447387
- Makhenko, V. I.; Pochynok, V. E. 2006. *Strength Calculation of Welded Joints with Crack-Like Imperfections*. Kiev: E. O. Paton Electric Welding Institute. 266 p. ISBN 966-8872-02-9.
- Медведев, С. В. 2001. Компьютерное моделирование остаточных сварочных деформаций при технологическом проектировании сварочных конструкций [Medvedev, S. V. Computer modeling of residual welding deformations beside technological designing of welding constructions], *Сварочное производство* [Welding production] 8: 10–17.
- Outinen, J.; Kaitila, O.; Mäkeläinen, P. 2001. *High-temperature Testing of Structural Steel and Modelling of Structures at Fire Temperatures*. Research Report. Helsinki University of Technology.
- Teng, T.-L.; Fung, Ch.-P.; Chang, P.-H. 2002. Effect of Weld Geometry and Residual Stresses of Fatigue in Butt-welded Joints, *International Journal of Pressure Vessels and Piping* 79 (1): 467–482. doi:10.1016/S0308-0161(02)00060-1
- Wimporoy, R. C.; May, P. S.; O'Dowd, N. P.; Webster, G. A.; Smith, D. J.; Kingston, E. 2003. Measurement of Residual Stresses in T-Plate Weldments, *Journal of Strain Analysis for Engineering Design* 38(4): 349–365. doi:10.1243/03093240360692931
- Ziari, H.; Keymanesh, M.-R.; Khabiri, M. M. 2007. Finite-Element Modelling of Crack Sealant Flexible Pavement, *The Baltic Journal of Road and Bridge Engineering* 2(2): 89–93.

Received 17 August 2008; accepted 7 January 2010